Prompt J/ψ production in the Regge limit of QCD: From Tevatron to LHC

V.A. Saleev*

II. Institut für Theoretische Physik, Universität Hamburg,

Luruper Chaussee 149, 22761 Hamburg, Germany and

Samara State University, Academic Pavlov Street 1, 443011 Samara, Russia

M.A. Nefedov† and A.V. Shipilova‡

Institut f. Kernphysik, Forschungszentrum Juelich, 52425 Juelich, Germany and

Samara State University, Academic Pavlov Street 1, 443011 Samara, Russia

Abstract

We study prompt $J/\psi-$meson hadroproduction invoking the hypothesis of gluon Reggeization in $t-$channel exchanges at high energy and the factorization formalism of nonrelativistic quantum chromodynamics at the leading order in the strong-coupling constant α_s and the relative velocity of quarks v. The transverse-momentum distribution of direct and prompt $J/\psi-$meson production measured at the Fermilab Tevatron fitted to obtain the nonperturbative long-distance matrix elements, which are used to predict prompt J/ψ production spectra at the CERN LHC. At the numerical calculation, we adopt the Kimber-Martin-Ryskin and Blümlein prescriptions to derive unintegrated gluon distribution function of the proton from their collinear counterpart, for which we use the Martin-Roberts-Stirling-Thorne set. Without adjusting any free parameters, we find good agreement with measurements by the ATLAS, CMS and LHCb Collaborations at the LHC at the hadronic c.m. energy $\sqrt{S} = 7$ TeV.

PACS numbers: 12.38.-t,12.40.Nn,13.85.Ni,14.40.Gx

*Electronic address: saleev@ssu.samara.ru, saleev@mail.desy.de

†Electronic address: nefedovma@gmail.com

‡Electronic address: alexshipilova@ssu.samara.ru

I. INTRODUCTION

The production of heavy quarkonium at hadron colliders provides useful laboratory for testing the high-energy limit of quantum chromodynamics (QCD) as well as the interplay of perturbative and nonperturbative phenomena in QCD.

The total collision energies, $\sqrt{S} = 1.8$ TeV and 1.96 TeV in Tevatron Runs I and II, respectively, and $\sqrt{S} = 7$ TeV or 14 TeV at the LHC, sufficiently exceed the characteristic scale μ of the relevant hard processes, which is of order of quarkonium transverse mass $M_T = \sqrt{M^2 + p_T^2}$, *i.e.* we have $\Lambda_{\rm QCD} \ll \mu \ll \sqrt{S}$. In this high-energy regime, so called "Regge limit", the contribution of partonic subprocesses involving t-channel parton (gluon or quark) exchanges to the production cross section can become dominant. Then the transverse momenta of the incoming partons and their off-shell properties can no longer be neglected, and we deal with "Reggeized" t-channel partons. These $t-$channel exchanges obey multi-Regge kinematics (MRK), when the particles produced in the collision are strongly separated in rapidity. If the same situation is realized with groups of particles, then quasi-multi-Regge kinematics (QMRK) is at work. In the case of $J/\psi-$meson inclusive production, this means the following: $J/\psi-$meson (MRK) or J/ψ-meson plus gluon jet (QMRK) is produced in the central region of rapidity, while other particles are produced with large modula of rapidities.

The parton Reggeization approach (PRA) [1, 2] is particularly appropriate for high-energy phenomenology. We see, the assumption of a dominant role of MRK or QMRK production mechanisms at high energy works well. PRA is based on an effective quantum field theory implemented with the non-Abelian gauge-invariant action including fields of Reggeized gluons [3] and Reggeized quarks [4]. Reggeized partons interact with quarks and Yang-Mills gluons in a specific way. Recently, in Ref.[5], the Feynman rules for the effective theory of Reggeized gluons were derived for the induced and some important effective vertices. This approach was successfully applied to interpret the production of isolated jets [6], prompt photons [7], diphotons [8], charmed mesons [9], bottom-flavored jets [10] measured at the Fermilab Tevatron, at the DESY HERA and at the CERN LHC, in the small-p_T regime, where $p_T << \sqrt{S}$. We suggest the MRK (QMRK) production mechanism to be the dominant one at small p_T values. Using the Feynman rules for the effective theory, we can construct heavy quarkonium production amplitudes in framework of non-relativistic QCD (NRQCD)[11, 12].

The factorization formalism of the NRQCD is a rigorous theoretical framework for the description of heavy-quarkonium production and decay. The factorization hypothesis of NRQCD assumes the separation of the effects of long and short distances in heavy-quarkonium production. NRQCD is organized as a perturbative expansion in two small parameters, the strong-coupling constant α_s and the relative velocity v of the heavy quarks inside a heavy quarkonium.

Our previous analysis of charmonium [13, 14] and bottomonium [14, 15] production at the Fermilab Tevatron using the high-energy factorization scheme and NRQCD approach has shown the efficiency of such type of high-energy phenomenology. In this paper we repeat our calculations for the direct and prompt $J/\psi-$meson transverse momentum spectra at the Fermilab Tevatron [13] to obtain by fitting procedure octet nonperturbative matrix elements (NMEs), than we calculate prompt $J/\psi-$meson spectra, which were measured recently at the CERN LHC Collider at the energy of $\sqrt{S} = 7$ TeV. We find a good agreement of our calculations and experimental data from ATLAS [16], CMS [17] and LHCb [18] Collaborations.

II. MODEL

Working at the leading order (LO) in α_s and v we consider the following partonic subprocesses, which describe charmonium production at high energy:

$$R(q_1) + R(q_2) \ \rightarrow \ \mathcal{H}[^3P_J^{(1)}, {}^3S_1^{(8)}, {}^1S_0^{(8)}, {}^3P_J^{(8)}](p), \tag{1}$$

$$R(q_1) + R(q_2) \ \rightarrow \ \mathcal{H}[^3S_1^{(1)}](p) + g(p'), \tag{2}$$

where R is the Reggeeized gluon and g is the Yang-Mills gluon, respectively, with four-momenta indicated in parentheses, $\mathcal{H}[n]$ is the physical charmonium state, $n = {}^{2S+1}L_J^{(1,8)}$ is the included $c\bar{c}$ Fock state with the spin S, total angular momentum J, orbital angular momentum L and in the singlet $^{(1)}$ or in the octet $^{(8)}$ color state.

In the general case, the partonic cross section of charmonium production receives from the $c\bar{c}$ Fock state $[n] = [^{2S+1}L_J^{(1,8)}]$ the contribution [11, 12]

$$d\hat{\sigma}(R + R \rightarrow c\bar{c}[^{2S+1}L_J^{(1,8)}] \rightarrow \mathcal{H}) = d\hat{\sigma}(R + R \rightarrow c\bar{c}[^{2S+1}L_J^{(1,8)}]) \frac{\langle \mathcal{O}^{\mathcal{H}}[^{2S+1}L_J^{(1,8)}] \rangle}{N_{\rm col} N_{\rm pol}}, \tag{3}$$

where $N_{\rm col} = 2N_c$ for the color-singlet state, $N_{\rm col} = N_c^2 - 1$ for the color-octet state, and $N_{\rm pol} = 2J + 1$, $\langle \mathcal{O}^{\mathcal{H}}[^{2S+1}L_J^{(1,8)}]\rangle$ are the NMEs. They satisfy the multiplicity relations

$$\begin{aligned}
\langle \mathcal{O}^{\psi(nS)}[^3P_J^{(8)}]\rangle &= (2J+1)\langle \mathcal{O}^{\psi(nS)}[^3P_0^{(8)}]\rangle,\\
\langle \mathcal{O}^{\chi_{cJ}}[^3P_J^{(1)}]\rangle &= (2J+1)\langle \mathcal{O}^{\chi_{c0}}[^3P_0^{(1)}]\rangle,\\
\langle \mathcal{O}^{\chi_{cJ}}[^3S_1^{(8)}]\rangle &= (2J+1)\langle \mathcal{O}^{\chi_{c0}}[^3S_1^{(8)}]\rangle,
\end{aligned} \tag{4}$$

which follow from heavy-quark spin symmetry to LO in v.

The partonic cross section of $c\bar{c}$ production is defined as

$$d\hat{\sigma}(R + R \to c\bar{c}[^{2S+1}L_J^{(1,8)}]) = \frac{1}{I}\overline{|\mathcal{A}(R + R \to c\bar{c}[^{2S+1}L_J^{(1,8)}])|^2}d\Phi, \tag{5}$$

where $I = 2x_1x_2S$ is the flux factor of the incoming particles, which is taken as in the collinear parton model [19], $\mathcal{A}(R + R \to c\bar{c}[^{2S+1}L_J^{(1,8)}])$ is the production amplitude, the bar indicates average (summation) over initial-state (final-state) spins and colors, and $d\Phi$ is the invariant phase space volume of the outgoing particles. This convention implies that the cross section in the high-energy factorization scheme is normalized approximately to the cross section for on-shell gluons in the collinear parton model when $\mathbf{q}_{1T} = \mathbf{q}_{2T} = \mathbf{0}$.

The LO results for the squared amplitudes of subprocesses (1) and (2) that we found by using the Feynman rules of Ref. [5] coincide with those we obtained in Ref. [13]. The formulas for the squared amplitudes $\overline{|\mathcal{A}(R + R \to c\bar{c}[^{2S+1}L_J^{(1,8)}])|^2}$ for the $2 \to 1$ subprocesses (1) are listed in Eq. (27) of Ref. [13]. The analytical result in case of the $2 \to 2$ subprocess (2) is presented in Ref.[14], where the results for the $2 \to 1$ subprocesses are also listed, but in another equivalent form. The relation between these forms is discussed in Ref.[15].

Exploiting the hypothesis of high-energy factorization, we may write the hadronic cross section $d\sigma$ as convolution of partonic cross section $d\hat{\sigma}$ with unintegrated parton distribution functions (PDFs) $\Phi_g^p(x, t, \mu^2)$ of Reggeized gluon in the proton, as

$$\begin{aligned}
d\sigma(p + p \to \mathcal{H} + X) = &\int \frac{dx_1}{x_1}\int \frac{d^2\mathbf{q}_{1T}}{\pi}\Phi_g^p\left(x_1, t_1, \mu^2\right)\int \frac{dx_2}{x_2}\int \frac{d^2\mathbf{q}_{2T}}{\pi}\\
&\times \Phi_g^p\left(x_2, t_2, \mu^2\right) d\hat{\sigma}(R + R \to \mathcal{H} + X).
\end{aligned} \tag{6}$$

$t_1 = |\mathbf{q}_{1T}|^2$, $t_2 = |\mathbf{q}_{2T}|^2$, x_1 and x_2 are the fractions of the proton momenta passed on to the Reggeized gluons, and the factorization scale μ is chosen to be of order M_T. The collinear and unintegrated gluon distribution functions are formally related as

$$xG^p(x, \mu^2) = \int^{\mu^2} \Phi_g^p(x, t, \mu^2)dt, \tag{7}$$

so that, for $\mathbf{q}_{1T} = \mathbf{q}_{2T} = \mathbf{0}$, we recover the conventional factorization formula of the collinear parton model,

$$d\sigma(p + p \to \mathcal{H} + X) = \int dx_1 G^p(x_1, \mu^2) \int dx_2 G^p(x_2, \mu^2) d\hat{\sigma}(g + g \to \mathcal{H} + X). \tag{8}$$

We now describe how to evaluate the differential hadronic cross section from Eq. (6) combined with the squared amplitudes of the $2 \to 1$ and $2 \to 2$ subprocesses (1) and (2), respectively. The rapidity and pseudorapidity of a charmonium state with four-momentum $p^\mu = (p^0, \mathbf{p}_T, p^3)$ are given by

$$y = \frac{1}{2} \ln \frac{p^0 + p^3}{p^0 - p^3}, \quad \eta = \frac{1}{2} \ln \frac{|\mathbf{p}| + p^3}{|\mathbf{p}| - p^3}, \tag{9}$$

respectively, and $dy = \dfrac{|\mathbf{p}|}{p^0} d\eta$.

The invariant phase volume $d\Phi$ in the Eq. (5) for $2 \to 1$ subprocess (1) can be presented as follows:

$$\begin{aligned} d\Phi(\mathbf{p}) &= (2\pi)^4 \delta^{(4)}(q_1 + q_2 - p) \frac{d^3p}{(2\pi)^3 2p^0} \\ &= \frac{4\pi^2 p_T}{S} \delta(\xi_1 - \frac{p^0 + p^3}{\sqrt{S}}) \delta(\xi_2 - \frac{p^0 - p^3}{\sqrt{S}}) \delta^2(\mathbf{q}_{1T} + \mathbf{q}_{2T} - \mathbf{p}_T) dp_T dy. \end{aligned} \tag{10}$$

From the Eqs. (5), (6) and (10) we obtain the master formula for the $2 \to 1$ subprocess (1):

$$\begin{aligned} \frac{d\sigma(p + p \to \mathcal{H} + X)}{dp_T dy} &= \frac{p_T}{(p_T^2 + M^2)^2} \int dt_1 \int d\varphi_1 \\ &\times \Phi_g^p(\xi_1, t_1, \mu^2) \Phi_g^p(\xi_2, t_2, \mu^2) \overline{|\mathcal{A}(R + R \to \mathcal{H})|^2}, \end{aligned} \tag{11}$$

where $t_2 = t_1 + p_T^2 - 2p_T \sqrt{t_1} \cos(\phi_1)$ and the relation $\xi_1 \xi_2 S = p_T^2 + M^2$ has been taken into account.

The invariant phase volume $d\Phi$ in the Eq. (5) for $2 \to 2$ subprocess (2) can be presented as follows:

$$\begin{aligned} d\Phi(\mathbf{p}, \mathbf{p}') &= (2\pi)^4 \delta^{(4)}(q_1 + q_2 - p - p') \frac{d^3p}{(2\pi)^3 2p^0} \frac{d^3p'}{(2\pi)^3 2p'^0} \\ &= \frac{p_T}{4\pi} \delta((q_1 + q_2 - p)^2) dp_T dy. \end{aligned} \tag{12}$$

Such a way, accordingly the Eqs. (5), (6) and (12), we have the master formula for the $2 \to 2$ subprocess (2):

$$\begin{aligned} \frac{d\sigma(p + p \to \mathcal{H} + X)}{dp_T dy} &= \frac{p_T}{(2\pi)^3} \int dt_1 \int d\varphi_1 \int dx_2 \int dt_2 \int d\varphi_2 \\ &\times \Phi_g^p(x_1, t_1, \mu^2) \Phi_g^p(x_2, t_2, \mu^2) \frac{\overline{|\mathcal{A}(R + R \to \mathcal{H} + g)|^2}}{(x_2 - \xi_2)(2x_1 x_2 S)^2}, \end{aligned} \tag{13}$$

where $\phi_{1,2}$ are the angles enclosed between $\vec{\mathbf{q}}_{1,2T}$ and the transverse momentum $\vec{\mathbf{p}}_T$ of $\mathcal{H}$,

$$x_1 = \frac{1}{(x_2 - \xi_2)S}\left[(\mathbf{q}_{1T} + \mathbf{q}_{2T} - \mathbf{p}_T)^2 - M^2 - |\mathbf{p}_T|^2 + x_2\xi_1 S\right]. \tag{14}$$

In our numerical analysis, we adopt as our default the prescription proposed by Kimber, Martin, and Ryskin (KMR) [20] to obtain unintegrated gluon PDF of the proton from the conventional integrated one, as implemented in Watt's code [21]. As is well known [22], other popular prescriptions, such as those by Blümlein [23] or by Jung and Salam [24], produce unintegrated PDFs with distinctly different t dependences. In order assess the resulting theoretical uncertainty, we also evaluate the unintegrated gluon PDF using the Blümlein approach, which resums small-x effects according to the Balitsky-Fadin-Kuraev-Lipatov (BFKL) equation [3]. As input for these procedures, we use the LO set of the Martin-Roberts-Stirling-Thorne (MRST) [25, 26] proton PDF as our default.

Throughout our analysis the renormalization and factorization scales are identified and chosen to be $\mu = \xi M_T$, where ξ is varied between 1/2 and 2 about its default value 1 to estimate the theoretical uncertainty due to the freedom in the choice of scales. The resulting errors are indicated as shaded bands in the figures.

III. RESULTS

At first, we examine direct and prompt (sum of direct production, production via radiative decays of χ_{cJ} mesons and production via decays of ψ' mesons contributions) $J/\psi-$meson production in proton-antiproton collisions at the Tevatron at the energies $\sqrt{S} = 1.8$ TeV (Run I)[27] and $\sqrt{S} = 1.96$ TeV (Run II)[28] in the central region of pseudorapidity $|\eta| < 0.6$. The data of Run II includes p_T distributions of prompt J/ψ mesons, so far without separation into direct, $\chi_{cJ}-$decay, and $\psi'-$decay contributions. In the Ref.[13], we have performed a joint fit to the Run I and Run II CDF data [27, 28] to obtain the color-octet NME's for J/ψ, ψ', and χ_{cJ} mesons. Our fits included five experimental data sets, which come as p_T distributions of J/ψ mesons from direct production, prompt production, χ_{cJ} decays, and ψ' decays. Since in the previous calculations we have used the old set MRST98 [25] as a collinear input for unintegrated PDF, in the present study we repeat our fit with the next-generation MRST set [26]. We find small differences between the old and new fit parameters, however, it is important for precise description of the data. The results of our fit are presented in

the Table I along with results of the fit in the next to leading order (NLO) of collinear parton model (PM) and NRQCD approach [31]. Oppositely the Ref.[31], we perform a fit procedure by assumption for NMEs to be only positive. Than, using the CDF data for a prompt J/ψ production [27], presented separately for direct J/ψ mesons, J/ψ from ψ' decays, and J/ψ from χ_{cJ} decays, we obtain color-octet NMEs $\langle \mathcal{O}^{J/\psi}[^3S_1^{(8)}, ^1S_0^{(8)}, ^3P_0^{(8)}]\rangle$, $\langle \mathcal{O}^{\psi'}[^3S_1^{(8)}, ^1S_0^{(8)}, ^3P_0^{(8)}]\rangle$, and $\langle \mathcal{O}^{\chi_{c0}}[^3S_1^{(8)}]\rangle$ independently from each other.

Looking at the Table I, we find a good agreement with the NLO fit in collinear parton model performed in the Ref. [31], which strongly improves if we take into account that a sum of contributions of NMEs $\langle \mathcal{O}^{J/\psi}[^1S_0^{(8)}]\rangle$ and $\langle \mathcal{O}^{J/\psi}[^3P_0^{(8)}]\rangle$ from the Ref. [31], leading to almost parallel J/ψ transverse momenta spectra, corresponds to our contribution of the NME $\langle \mathcal{O}^{J/\psi}[^1S_0^{(8)}]\rangle$. Such an agreement demonstrates a validity of factorization in the charmonium production in hadronic collisions, i.e. an independence of the $c\bar{c}$ production mechanism from the nonperturbative charmonium formation at the last step. It is necessary to note that a same consent between LO results obtained in the uncollinear factorization scheme and NLO results obtained in the collinear parton model is also observed when describing other relevant processes, see Refs. [6–10].

In Figs. 1–4, we compare the CDF data on J/ψ mesons from direct production, ψ' decays and χ_{cJ} decays in Run I [27] and from prompt production in Run II [28], with the respective theoretical results evaluated with the NMEs listed in Table I. As default, we present in all figures the theoretical results which are obtained using KMR unintegrated gluon density [20]. The comparison between KMR [20] and Blümlein [23] PDFs is made in Fig. 4 for a prompt J/ψ production only.

In Fig. 1 one can find a dominance of color-octet contributions at all values of direct J/ψ meson transverse momentum: $[^3S_1^{(8)}]$ contribution dominates at the large values $p_T > 10$ GeV, and $[^1S_0^{(8)}]$ — at the small $p_T < 10$ GeV. The situation is very similar for J/ψ production from ψ' decay, considered in Fig. 2. It is also important, that the $[^3P_J^{(8)}]$ contribution vanishes in direct J/ψ and ψ' production. The obtained results are in agreement with previous calculations of Ref. [13] with a slight difference. In Ref. [29] it was also shown that in the direct J/ψ production at the Tevatron color-octet contribution dominates. Oppositely our conclusions, in Ref. [29], the main contribution comes from the $[^1S_0^{(8)}]$ NME at all transverse momenta. The reason of this discrepancy arises from the fact that in Ref. [29] the color-octet NMEs for J/ψ meson have been obtained by a fit of direct J/ψ production data for $p_T > 5$

GeV only. In our fit we take into account both direct [27] and prompt [28] J/ψ production data, the last ones contain points in a small p_T region. We observe, the inclusion of prompt J/ψ production data in the fit to change the relative weight of different color-octet NMEs. This fact should be important in study of polarized J/ψ mesons.

In case of J/ψ production via decays of χ_{cJ} mesons, considered in Fig. 3, we confirm the conclusion of Refs.[13, 30], which reads, that in the high-energy factorization scheme, the color-singlet contribution is sufficient to describe the data for production of $P-$wave charmonium states.

In Fig. 4, the p_T distribution of prompt J/ψ production in Tevatron Run II is presented as a sum of the contributions from direct production, ψ' decays, and χ_{cJ} decays. We observe at the $p_T \geq 2$ GeV the J/ψ mesons to be produced preferably directly. The contribution from χ_{cJ} decays dominates at small $p_T < 2$ GeV. The contribution from ψ' is smaller than other ones and it exceeds the contribution from χ_{cJ} decays only at the $p_T > 16$ GeV.

The curve number (5) in Fig. 4 is obtained using Blümlein unPDF [23]. The visible difference between this curve and the curve (4), which is obtained using KMR unPDF [20], takes place only in the region of small J/ψ transverse momentum. In the range of $p_T \geq 5$ GeV, there is no difference between them as in the prompt production as in the direct production or in the production via decays of high charmonium states, ψ' and χ_{cJ}.

As it is obvious from Figs. 1–4, the theoretical uncertainties associated with the variation of the factorization scale μ are large at the small p_T region, taking a value of about factor 5 between upper and lower boundaries, and they sufficiently decrease down to a factor 2 at the $p_T \geq 6$ GeV. The uncertainties from errors in the color-octet NMEs are small, they are about 7-10%.

Moving on from Tevatron to the LHC, which is currently running at the total energy being about 3.5 times larger than at the Tevatron, we expect the range of validity of our approach to be extended by the same factor, to $p_T \leq 70$ GeV, as we describe well the Tevatron data at the range of $0 < p_T < 20$ GeV. This expectation is nicely confirmed in Figs. 5–6, where the recent measurements of the prompt J/ψ production by the ATLAS Collaboration at the CERN LHC [16], which cover the kinematic region 1 GeV $< p_T <$ 70 GeV and $|y| < 2.4$, are compared with our predictions based on the particle Reggeization approach and NRQCD formalism. The measurements of the CMS Collaboration [17] were performed in the similar kinematic range 6.5 GeV $< p_T <$ 30 GeV and $|y| < 2.4$, see Fig. 7. We observe a dominant

role of direct production mechanism in the prompt J/ψ hadroproduction at the all values of J/ψ meson transverse momentum. Concerning the relative contributions of ψ' decays and χ_{cJ} decays into a prompt J/ψ production, we found the contribution from ψ' decays to dominate at the large $p_T > 20$ GeV, and the contribution from χ_{cJ} decays to dominate at the small p_T, respectively. Additionally, we compare our predictions with the data from LHCb Collaboration [18], which were extracted in the range $0 < p_T < 14$ GeV and $2 < |y| < 4.5$. We find a good agreement between our predictions and prompt J/ψ production data at the moderate rapidity interval $2.0 < |y| < 3.5$, see Figs. 8–9. At the same time our theoretical result overestimates the data of at most factor 2 in the range of large rapidity $3.5 < |y| < 4.5$. This distinction is expected in the parton Reggeization approach, because the multi-Regge kinematics conditions to be broken if J/ψ mesons are produced with large rapidity.

We observe, in Fig. 10, that relative contributions of the color-singlet (curve 1) and color-octet (curve 2) production mechanisms to the prompt J/ψ spectrum strongly depend on the J/ψ transverse momentum. Similarly to the NLO calculations in the collinear parton model, the color-octet contribution dominates at the large p_T region, basically via the contributions of the color-octet NMEs $\langle \mathcal{O}^{J/\psi}[^3S_1^{(8)}] \rangle$ and $\langle \mathcal{O}^{\psi'}[^3S_1^{(8)}] \rangle$. It is significant, the experimental data [16–18] depend on the assumption of polarization of produced J/ψ mesons slightly. We perform calculations and make a comparison to the data in a case of non-polarized J/ψ meson production.

Comparing our results with the recent studies of J/ψ meson hadroproduction in the conventional collinear PM, which were performed in full NLO approximation of NRQCD formalism [31] or in the non-complete NNLO* approximation of color-singlet model [32], we should emphasize the following. At first, oppositely to NLO and NNLO* calculations, which provide a good description of data only at non-small $p_T > 5$ GeV, we can reproduce data well at all transverse momenta p_T. At second, the present study along with the previous investigations in the parton Reggeization approach [6–10, 13–15, 29, 30] demonstrate the important role of (quasi)multi-Regge kinematics in particle production at high energies, this feature is out of account in the collinear PM. Such a way, we find the approach based on the effective theory of Reggeized partons [2, 3] and high-energy factorization scheme with unintegrated PDFs, which in the large logarithmic terms $(\ln(\mu^2/\Lambda^2_{QCD}),\ \ln(S/\mu^2))$ are resummed in all orders of strong coupling constant α_s, to be more adequate for the description of experimental data than fixed order in α_s calculations in the frameworks of

collinear PM.

IV. CONCLUSIONS

The Fermilab Tevatron and, even more so, the CERN LHC are currently probing particle physics at terascale c.m. energies $\sqrt{S}$, so that the hierarchy $\Lambda_{\rm QCD} \ll \mu \ll \sqrt{S}$, which defines the MRK and QMRK regimes, is satisfied for processes of heavy quark and heavy quarkonium production in the central region of rapidity, where μ is of order of their transverse mass. In this paper, we studied QCD processes of particular interest, namely prompt J/ψ hadroproduction, at LOs in the parton Reggeization approach and NRQCD approach, in which they are mediated by $2 \to 1$ and $2 \to 2$ partonic subprocesses initiated by Reggeized gluon collisions.

We found by the fit of Tevatron data that numerical values of the color-octet NMEs are very similar to ones obtained in the full NLO calculations based on NRQCD approach [31]. Using these NMEs, we nicely described recent LHC data for prompt J/ψ meson production measured by ATLAS [16], CMS [17] and LHCb [18] Collaborations at the whole presented range of J/ψ transverse momenta. We found only one exclusion, the region of large modulo of rapidity $|y| > 3.5$, where LHCb data are by a factor 2 smaller than our predictions. However, this kinematical region is out of the applicability limits of the MRK or QMRK pictures. Here and in Refs. [6–10, 13–15, 29, 30], parton Reggeization approach was demonstrated to be a powerful tool for the theoretical description of QCD processes in the high-energy limit.

V. ACKNOWLEDGEMENTS

We are grateful to B. A. Kniehl, M. Butenschön, M. Büscher and N. N. Nikolaev for useful discussions. The work of M. A. N. and A. V. S. was supported by the Federal Ministry for Science and Education of the Russian Federation under Contract No. 14.740.11.0894 and in part by the Grant DFG 436 RUS 113/940; the work of V. A. S. was supported in part by the Russian Foundation for Basic Research under Grant 11-02-00769-a and by SFB Fellowship of Hamburg University (SFB-676).

[1] V. S. Fadin and L. N. Lipatov, Nucl. Phys. **B406**, 259 (1993); **B477**, 767 (1996) [arXiv:hep-ph/9602287].

[2] L. N. Lipatov, Nucl. Phys. **B452**, 369 (1995) [arXiv:hep-ph/9502308].

[3] L. N. Lipatov, Sov. J. Nucl. Phys. **23**, 338 (1976) [Yad. Fiz. **23**, 642 (1976)]; E. A. Kuraev, L. N. Lipatov, and V. S. Fadin, Sov. Phys. JETP **44**, 443 (1976) [Zh. Eksp. Teor. Fiz. **71**, 840 (1976)]; Sov. Phys. JETP **45**, 199 (1977) [Zh. Eksp. Teor. Fiz. **72**, 377 (1977)]; I. I. Balitsky and L. N. Lipatov, Sov. J. Nucl. Phys. **28**, 822 (1978) [Yad. Fiz. **28**, 1597 (1978)]; Sov. Phys. JETP **63**, 904 (1986) [Zh. Eksp. Teor. Fiz. **90**, 1536 (1986)].

[4] L. N. Lipatov and M. I. Vyazovsky, Nucl. Phys. **B597**, 399 (2001) [arXiv:hep-ph/0009340].

[5] E. N. Antonov, L. N. Lipatov, E. A. Kuraev, and I. O. Cherednikov, Nucl. Phys. **B721**, 111 (2005) [arXiv:hep-ph/0411185].

[6] B. A. Kniehl, V. A. Saleev, A. V. Shipilova, E. V. Yatsenko, Phys. Rev. **D84** (2011) 074017. [arXiv:1107.1462 [hep-ph]].

[7] V. A. Saleev, Phys. Rev. D **78**, 034033 (2008) [arXiv:0807.1587 [hep-ph]]; Phys. Rev. D **78**, 114031 (2008) [arXiv:0812.0946 [hep-ph]].

[8] V. A. Saleev, Phys. Rev. D **80**, 114016 (2009) [arXiv:0911.5517 [hep-ph]].

[9] B. A. Kniehl, A. V. Shipilova, and V. A. Saleev, Phys. Rev. D **79**, 034007 (2009) [arXiv:0812.3376 [hep-ph]].

[10] B. A. Kniehl, V. A. Saleev, and A. V. Shipilova, Phys. Rev. D **81**, 094010 (2010) [arXiv:1003.0346 [hep-ph]]; PoS(DIS2010), 177 (2010); in Proceedings of Physics at the LHC 2010 (PLHC2010), Hamburg, Germany, 2010, edited by M. Diehl, J. Haller, T. Schörner-Sadenius, and G. Steinbrueck, DOI: `http://dx.doi.org/10.3204/DESY-PROC-2010-01/shipilova`.

[11] G. T. Bodwin, E. Braaten, and G. P. Lepage, Phys. Rev. D **51**, 1125 (1995); **55**, 5853(E) (1997).

[12] F. Maltoni, M. L. Mangano, and A. Petrelli, Nucl. Phys. **B519**, 361 (1998).

[13] B. A. Kniehl, D. V. Vasin, and V. A. Saleev, Phys. Rev. D **73**, 074022 (2006) [arXiv:hep-ph/0602179]; in Proceedings of the 15th International Workshop on Deep-Inelastic Scattering and Related Subjects (DIS 2007), Munich, Germany, 2007, edited by G. Grind-

hammer and K. Sachs, DOI: http://dx.doi.org/10.3360/dis.2007.169.

[14] D. V. Vasin, V. A. Saleev, Phys. Part. Nucl. **38** (2007) 635-658.

[15] B. A. Kniehl, V. A. Saleev, and D. V. Vasin, Phys. Rev. D **74**, 014024 (2006) [arXiv:hep-ph/0607254].

[16] G. Aad *et al.* [ATLAS Collaboration], Nucl. Phys. B **850** (2011) 387 [arXiv:1104.3038 [hep-ex]].

[17] V. Khachatryan *et al.* [CMS Collaboration], Eur. Phys. J. C **71** (2011) 1575 [arXiv:1011.4193 [hep-ex]].

[18] R. Aaij *et al.* [LHCb Collaboration], Eur. Phys. J. C **71** (2011) 1645 [arXiv:1103.0423 [hep-ex]].

[19] J. C. Collins and R. K. Ellis, Nucl. Phys. **B360**, 3 (1991).

[20] M. A. Kimber, A. D. Martin, and M. G. Ryskin, Eur. Phys. J. C **12**, 655 (2000) [arXiv:hep-ph/9911379]; Phys. Rev. D **63**, 114027 (2001) [arXiv:hep-ph/0101348]; G. Watt, A. D. Martin, and M. G. Ryskin, Eur. Phys. J. C **31**, 73 (2003) [arXiv:hep-ph/0306169]; Phys. Rev. D **70**, 014012 (2004); **70**, 079902(E) (2004) [arXiv:hep-ph/0309096].

[21] G. Watt, URL: http://gwatt.web.cern.ch/gwatt/.

[22] Small-x Collaboration, B. Andersson *et al.*, Eur. Phys. J. C **25**, 77 (2002) [arXiv:hep-ph/0204115]; F. Hautmann and H. Jung, Nucl. Phys. B (Proc. Suppl.) **184**, 64 (2008) [arXiv:0712.0568 [hep-ph]].

[23] J. Blümlein, Preprint DESY 95–121 (1995) [arXiv:hep-ph/9506403].

[24] H. Jung and G. P. Salam, Eur. Phys. J. C **19**, 351 (2001) [arXiv:hep-ph/0012143].

[25] A. D. Martin, R. G. Roberts, W. J. Stirling, and R. S. Thorne, Phys. Lett. B **531**, 216 (2002) [arXiv:hep-ph/0201127].

[26] A. D. Martin, W. J. Stirling, R. S. Thorne, Phys. Lett. **B636** (2006) 259-264. [hep-ph/0603143].

[27] F. Abe *et al.*,[CDF Collaboration], Phys. Rev. Lett. **79**, 572 (1997); **79**, 578 (1997); CDF Collaboration, T. Affolder *et al.*, Phys. Rev. Lett. **85**, 2886 (2000).

[28] D. Acosta *et al.*, [CDF Collaboration], Phys. Rev. D **71**, 032001 (2005).

[29] Ph. Hägler, R. Kirschner, A. Schäfer, L. Szymanowski, and O. V. Teryaev, Phys. Rev. D **63**, 077501 (2001) [arXiv:hep-ph/0008316].

[30] Ph. Hägler, R. Kirschner, A. Schäfer, L. Szymanowski, and O. V. Teryaev, Phys. Rev. Lett. **86**, 1446 (2001)[arXiv:hep-ph/0004263].

[31] M. Butenschoen and B. A. Kniehl, Phys. Rev. Lett. **106**, 022003 (2011) [arXiv:1009.5662

[hep-ph]]; Phys. Rev. D **84**, 051501 (2011) [arXiv:1105.0820 [hep-ph]].

[32] P. Artoisenet et al. Phys. Rev. Lett. **101**, 152001 (2008); J. P. Lansberg, Phys. Lett. B **695**, 149 (2011); E-print [arXiv:1107.0292].

[33] S. Brandt. Statistical and computational methods in data analysis. Heidelberg University, North Holland Publishing Company, 1970.

TABLE I: NMEs for J/ψ, ψ', and χ_{cJ} mesons from fits of the CDF data [27, 28] in the NLO collinear parton model [31] and in the parton Reggeization approach using the Blümlein [23], and KMR [20] unintegrated gluon distribution functions. The errors on our fit results are determined by the varying in turn each NME up and down about its central value until the value of χ^2 is increased by unity keeping all other NMEs fixed at their central values. When we obtained the value of χ^2/d.o.f. > 1, we have used normalizing multiplier approach [33] to reduce this value to unity.

NME	PM NLO [31]	Fit B	Fit KMR
$\langle \mathcal{O}^{J/\psi}[^3S_1^{(1)}]\rangle$/GeV^3	1.3	1.3	1.3
$\langle \mathcal{O}^{J/\psi}[^3S_1^{(8)}]\rangle$/GeV^3	$(1.68 \pm 0.46) \times 10^{-3}$	$(1.89 \pm 0.27) \times 10^{-3}$	$(2.23 \pm 0.27) \times 10^{-3}$
$\langle \mathcal{O}^{J/\psi}[^1S_0^{(8)}]\rangle$/GeV^3	$(3.04 \pm 0.35) \times 10^{-2}$	$(1.80 \pm 0.25) \times 10^{-2}$	$(1.84 \pm 0.19) \times 10^{-2}$
$\langle \mathcal{O}^{J/\psi}[^3P_0^{(8)}]\rangle$/GeV^5	$(-9.08 \pm 1.61) \times 10^{-3}$	0	0
χ^2/d.o.f	—	1.0	1.0
$\langle \mathcal{O}^{\psi'}[^3S_1^{(1)}]\rangle$/GeV^3	6.5×10^{-1}	6.5×10^{-1}	6.5×10^{-1}
$\langle \mathcal{O}^{\psi'}[^3S_1^{(8)}]\rangle$/GeV^3	$(1.88 \pm 0.62) \times 10^{-3}$	$(6.72 \pm 1.15) \times 10^{-4}$	$(9.33 \pm 1.62) \times 10^{-4}$
$\langle \mathcal{O}^{\psi'}[^1S_0^{(8)}]\rangle$/GeV^3	$(7.01 \pm 4.75) \times 10^{-3}$	$(3.63 \pm 1.40) \times 10^{-3}$	$(3.27 \pm 1.44) \times 10^{-3}$
$\langle \mathcal{O}^{\psi'}[^3P_0^{(8)}]\rangle$/GeV^5	$(-2.08 \pm 2.28) \times 10^{-3}$	0	0
χ^2/d.o.f	—	0.033	0.051
$\langle \mathcal{O}^{\chi_{c0}}[^3P_0^{(1)}]\rangle$/GeV^5	8.9×10^{-2}	8.9×10^{-2}	8.9×10^{-2}
$\langle \mathcal{O}^{\chi_{c0}}[^3S_1^{(8)}]\rangle$/GeV^3	—	$(2.14 \pm 0.67) \times 10^{-4}$	$(1.69 \pm 0.9) \times 10^{-4}$
χ^2/d.o.f	—	0.89	0.41

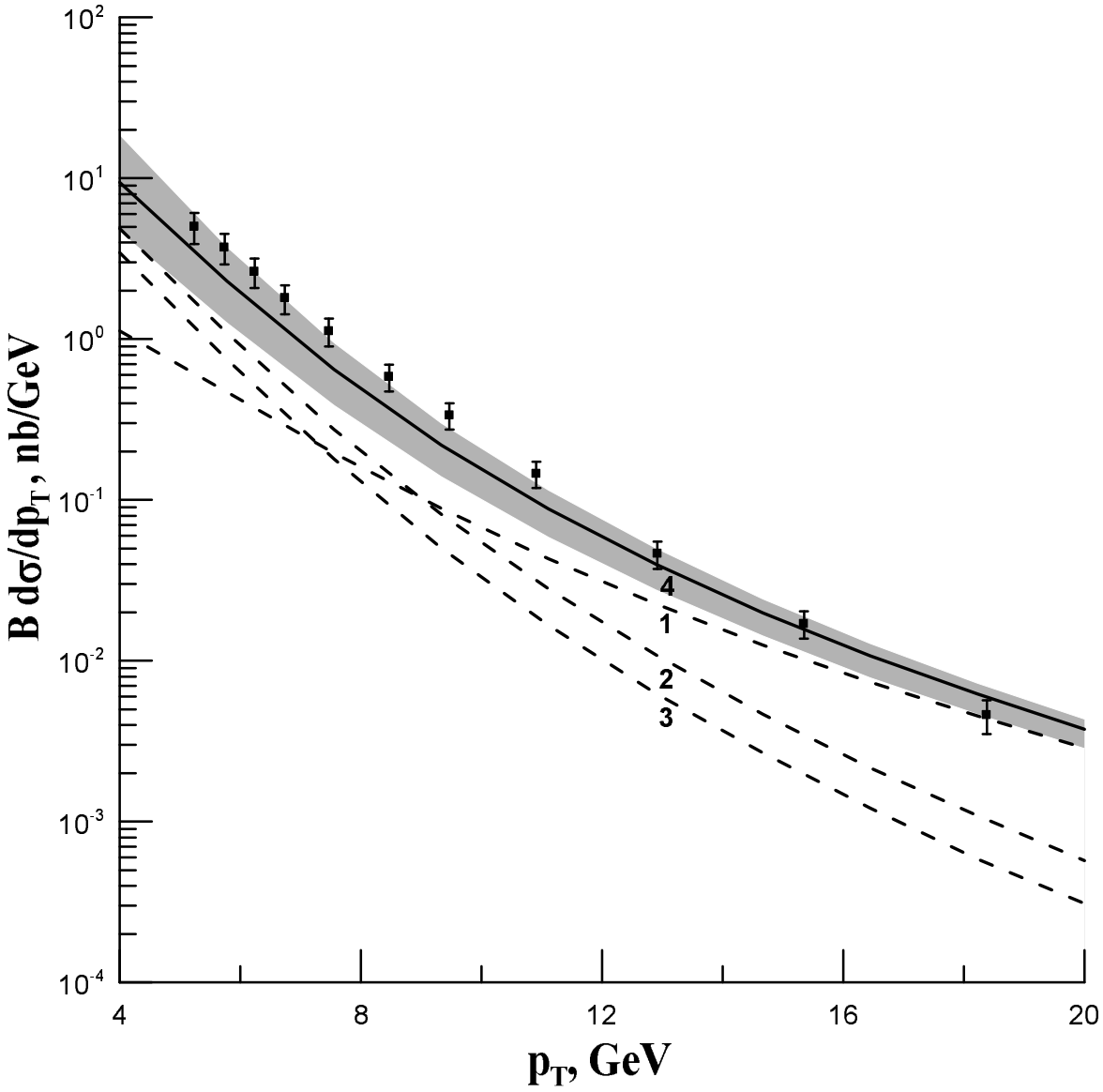

FIG. 1: Direct J/ψ transverse momentum spectrum from CDF Collaboration [27], $\sqrt{S} = 1.8$ TeV, $|\eta| < 0.6$, (1) is the contribution of $[^3S_1^{(8)}]$ state, (2) – $[^1S_0^{(8)}]$, (3) – $[^3S_1^{(1)}]$, (4) – sum of their all.

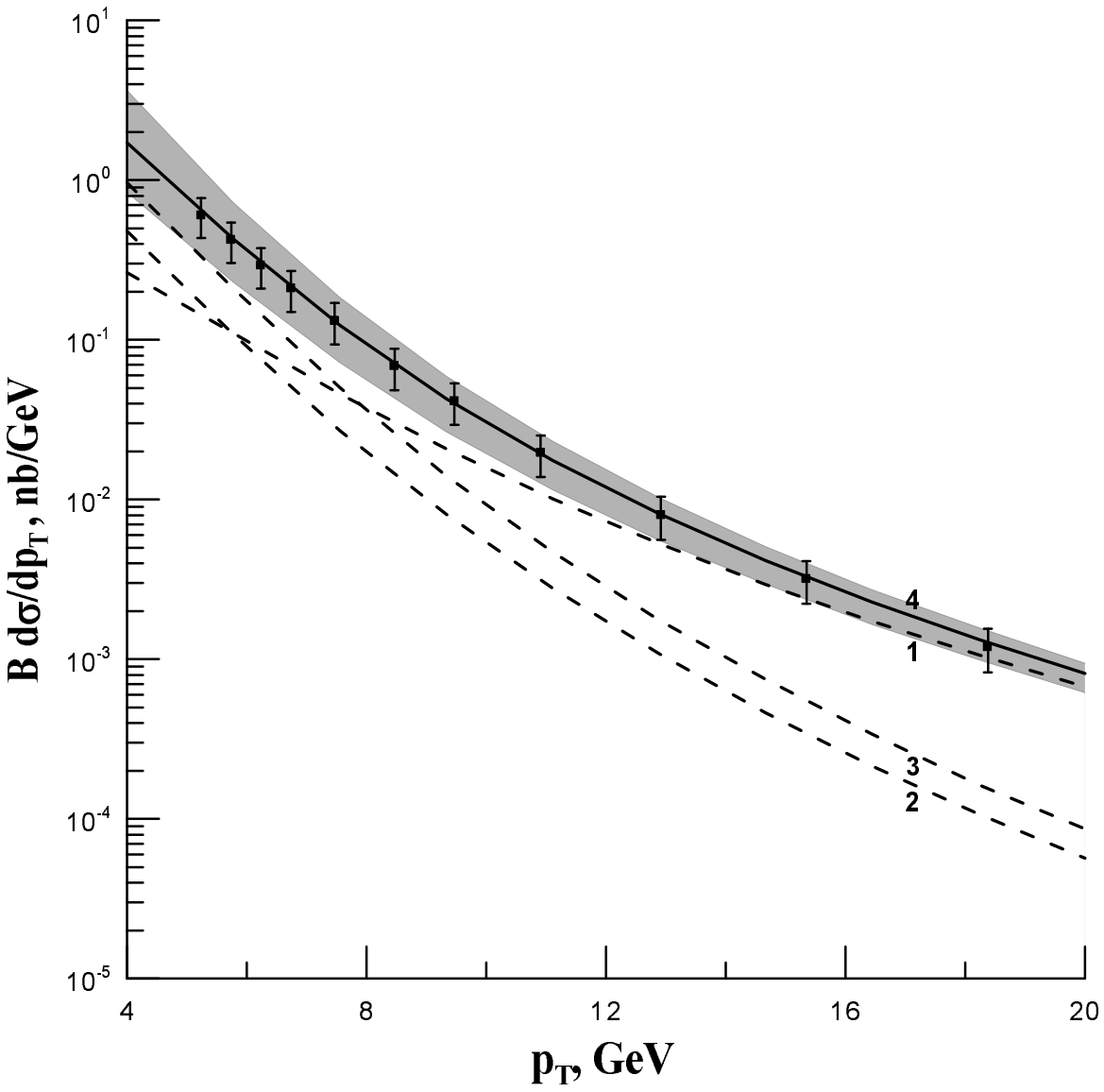

FIG. 2: J/ψ transverse momentum spectrum from ψ' decays from CDF Collaboration [27], $\sqrt{S} =$ 1.8 TeV, $|\eta| < 0.6$, (1) is the contribution of $[^3S_1^{(8)}]$ state, (2) – $[^3S_1^{(1)}]$, (3) – $[^1S_0^{(8)}]$, (4) – sum of their all.

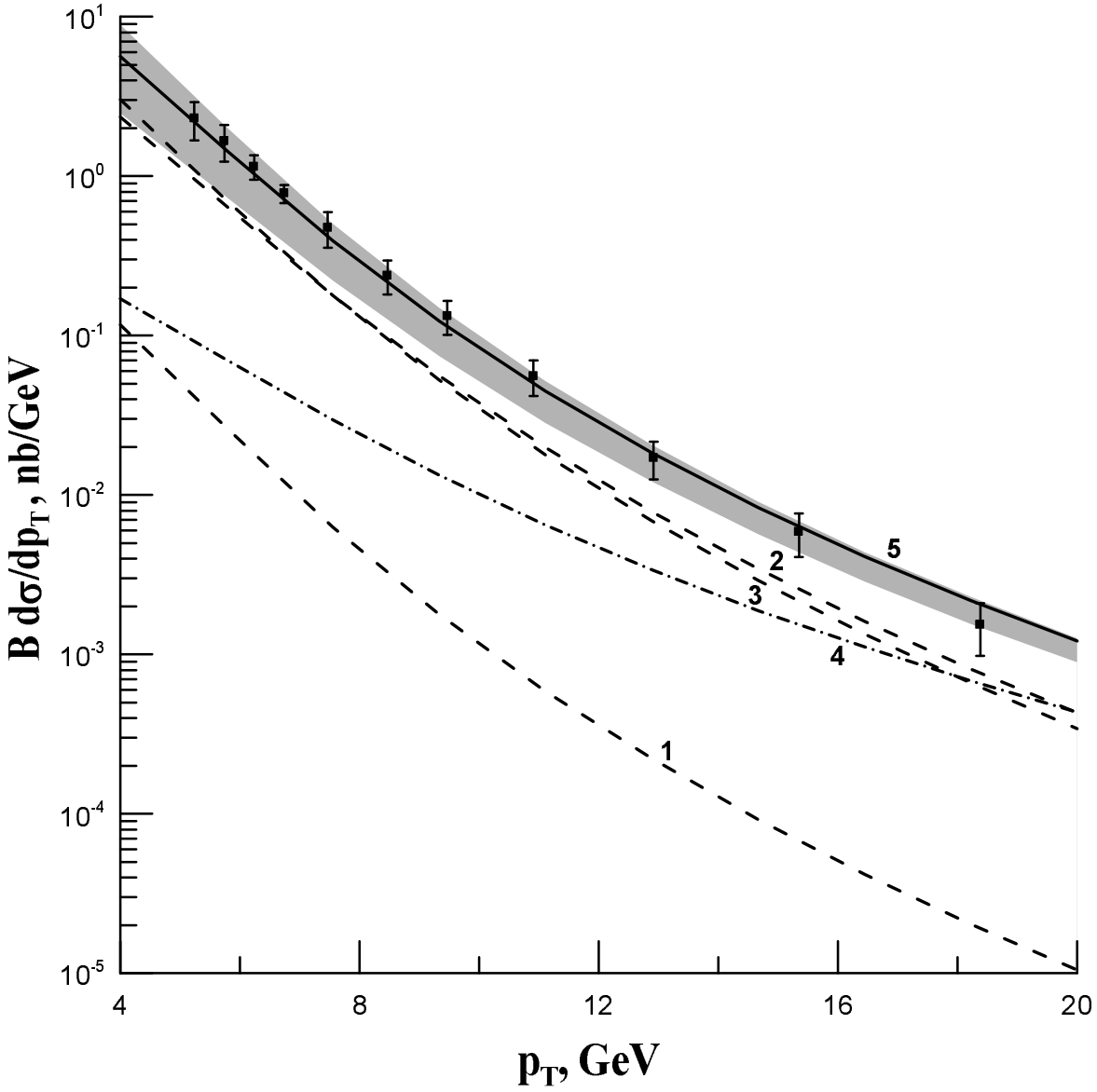

FIG. 3: J/ψ transverse momentum spectrum from χ_{cJ} decays from CDF Collaboration [27], $\sqrt{S} =$ 1.8 TeV, $|\eta| < 0.6$, (1) is the contribution of $[^3P_0^{(1)}]$ state, (2) – $[^3P_1^{(1)}]$, (3) – $[^3P_2^{(1)}]$, (4) – $[^3S_1^{(8)}]$, (5) – sum of their all.

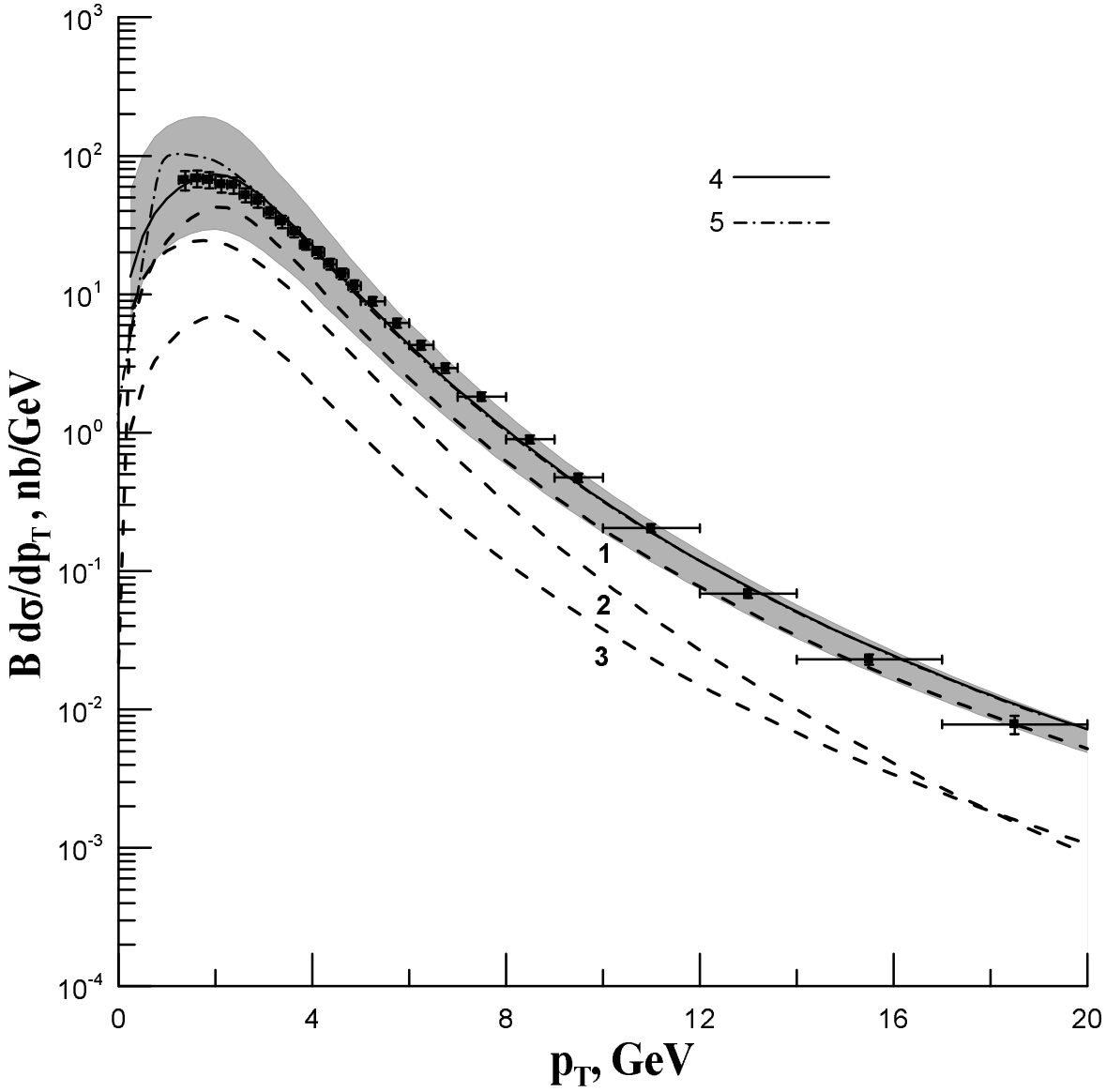

FIG. 4: Prompt J/ψ transverse momentum spectrum from CDF Collaboration [28], $\sqrt{S} = 1.96$ TeV, $|y| < 0.6$, (1) is the direct production, (2) – from χ_{cJ} decays, (3) – from ψ' decays, (4) – sum of their all (KMR unPDF), (5) – sum of all contributions (Blümlein unPDF).

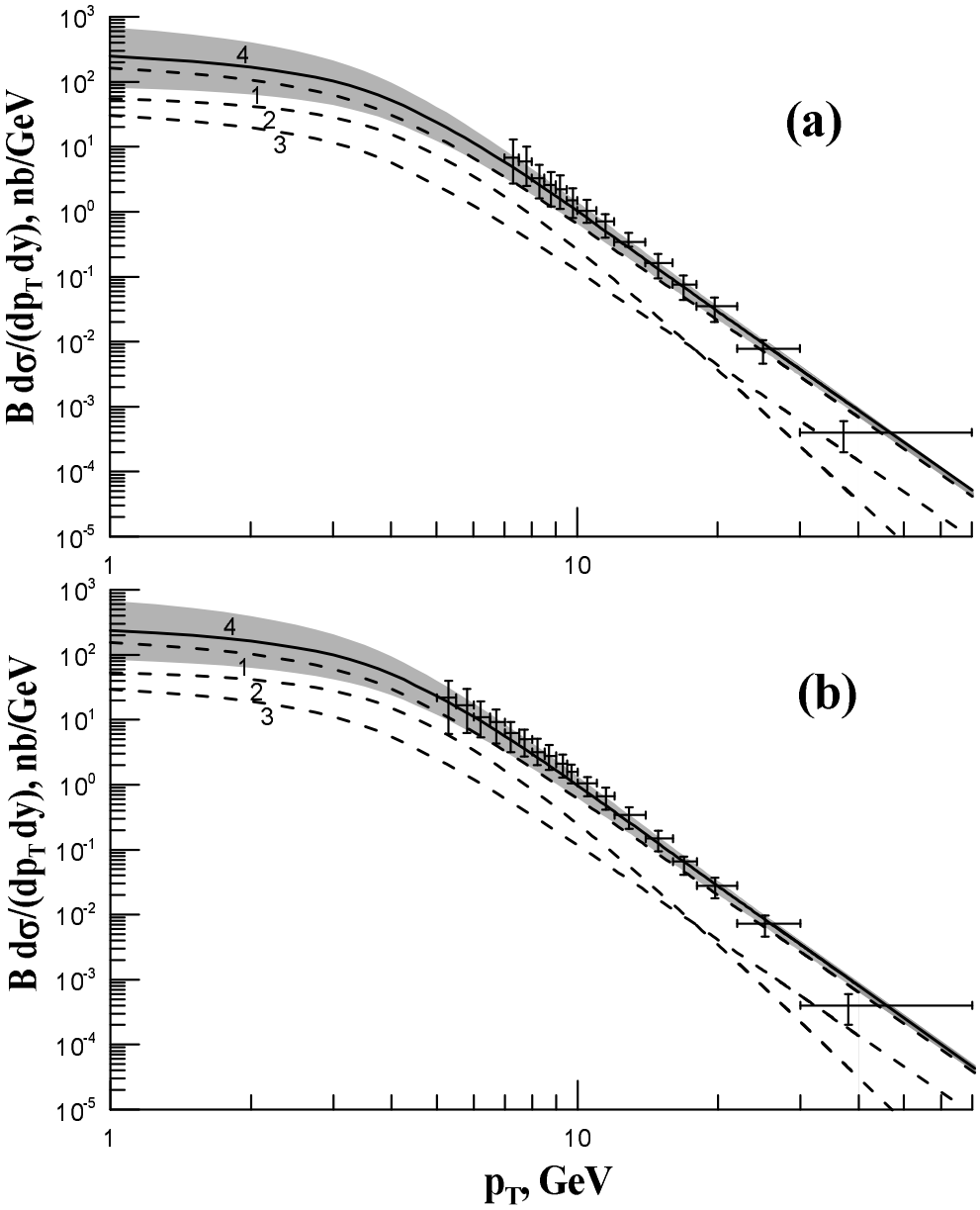

FIG. 5: Prompt J/ψ transverse momentum spectrum from ATLAS Collaboration [16], $\sqrt{S} = 7$ TeV, (1) is the direct production, (2) – from χ_{cJ} decays, (3) – from ψ' decays, (4) – sum of their all. For the different range in the rapidity: (a)– $|y| < 0.75$, (b) – $0.75 < |y| < 1.5$.

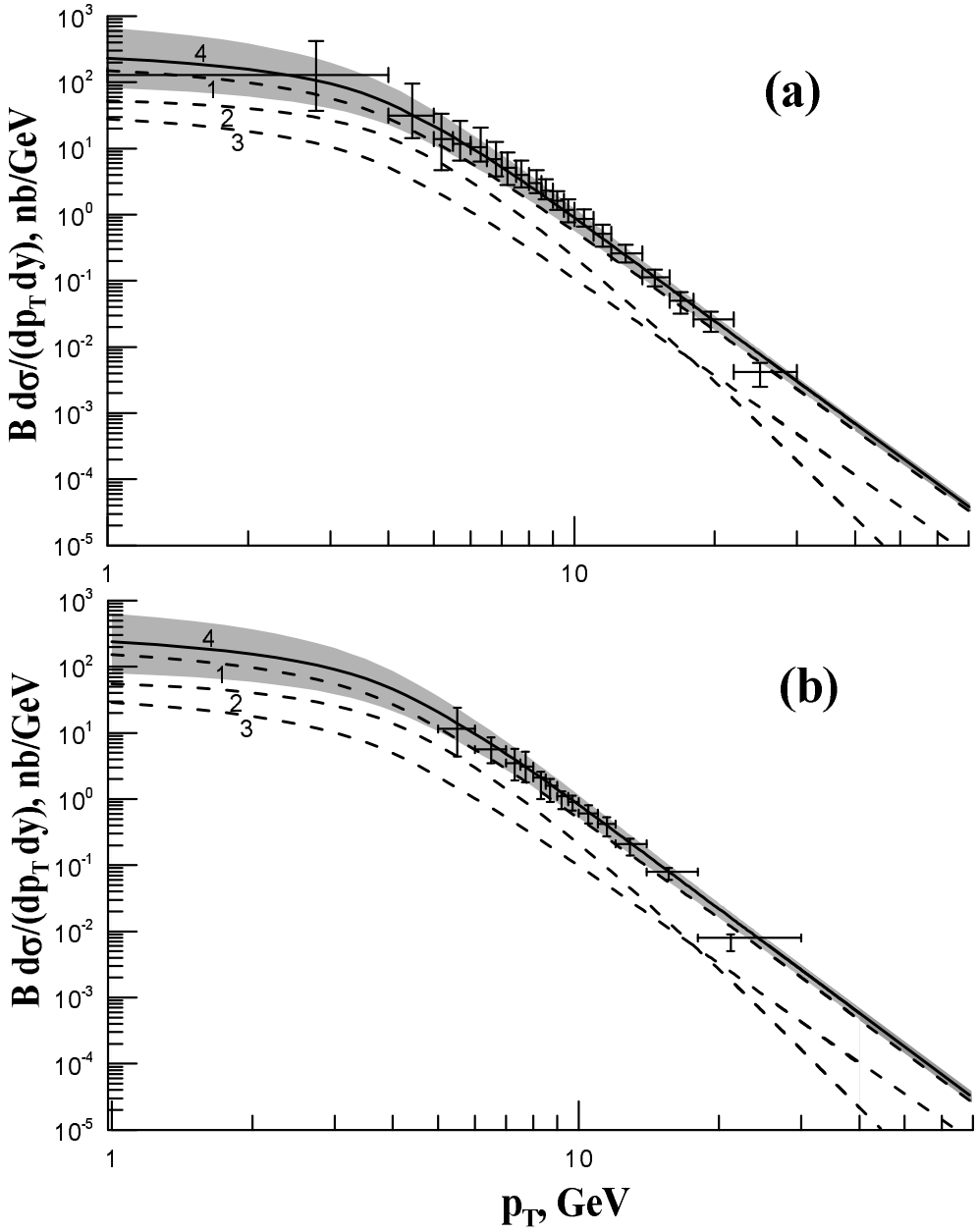

FIG. 6: Prompt J/ψ transverse momentum spectrum from ATLAS Collaboration [16], $\sqrt{S} = 7$ TeV, (1) is the direct production, (2) – from χ_{cJ} decays, (3) – from ψ' decays, (4) – sum of their all. For the different range in the rapidity: a) – $1.5 < |y| < 2.0$, (b) – $2.0 < |y| < 2.4$.

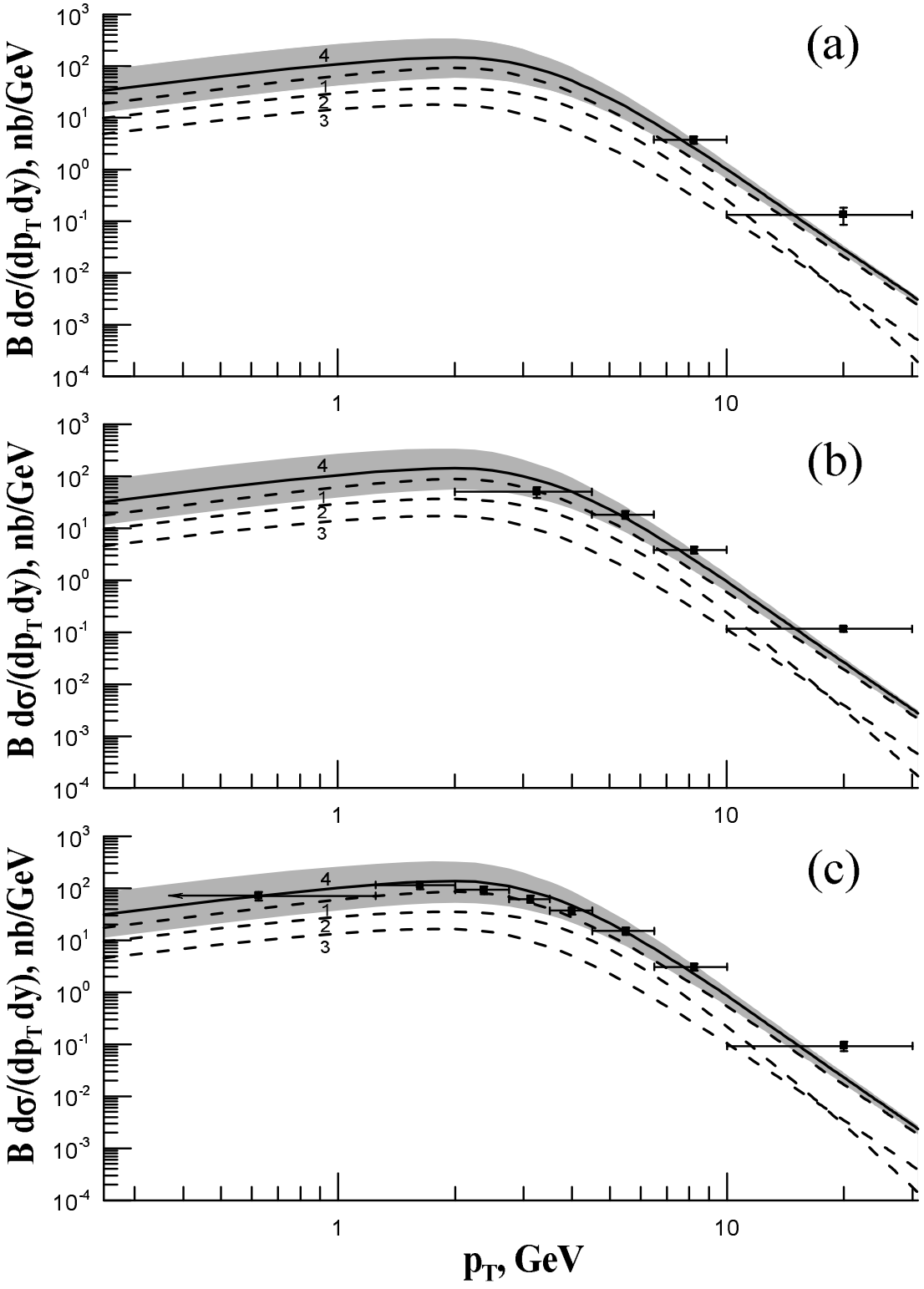

FIG. 7: Prompt J/ψ transverse momentum spectrum from CMS Collaboration [17], $\sqrt{S} = 7$ TeV, (1) is the direct production, (2) – from χ_{cJ} decays, (3) – from ψ' decays, (4) – sum of their all. For the different range in the rapidity: (a)– $|y| < 1.2$, (b) – $1.2 < |y| < 1.6$, (c) – $1.6 < |y| < 2.4$

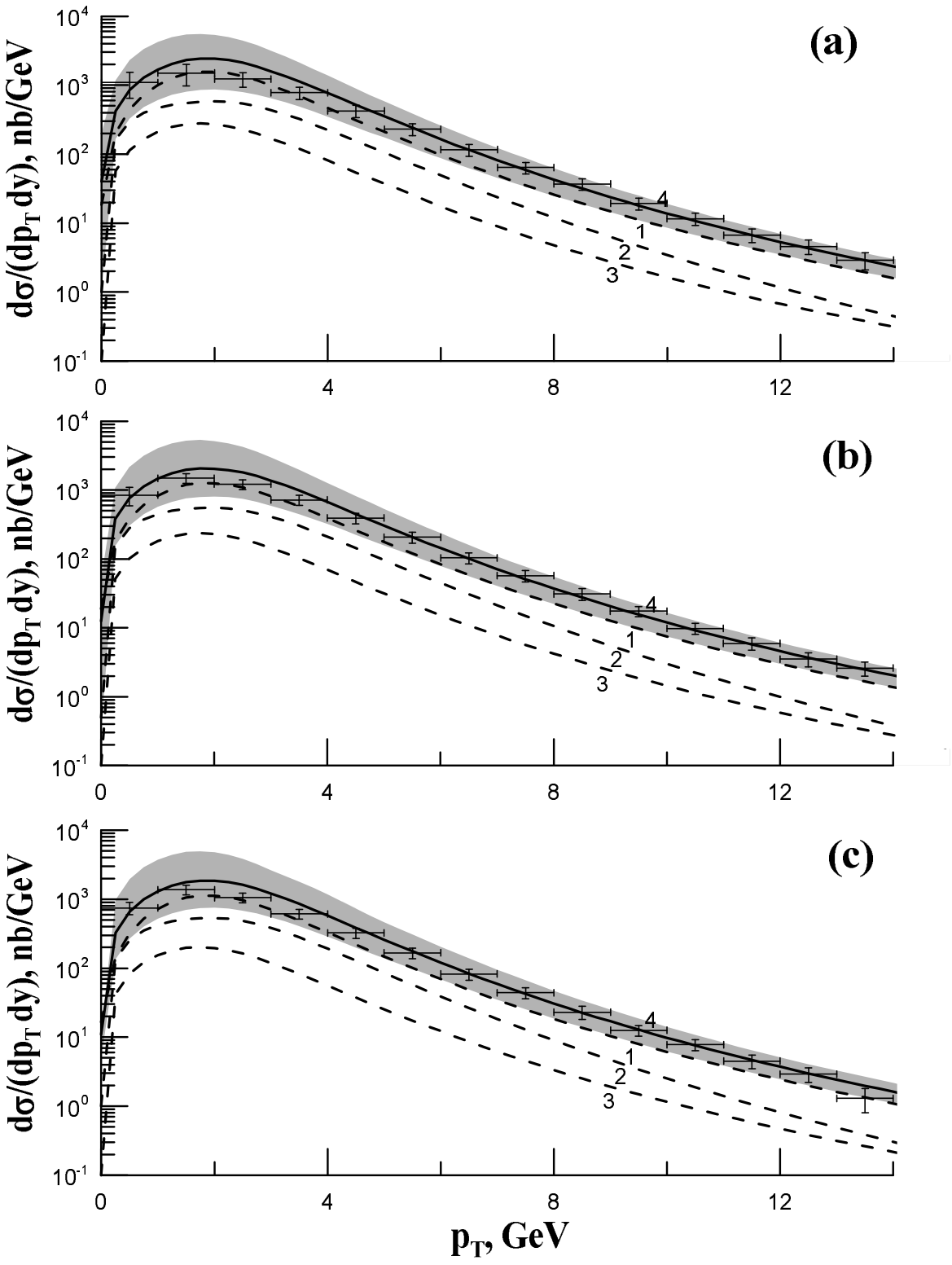

FIG. 8: Prompt J/ψ transverse momentum spectrum from LHCb Collaboration [18], $\sqrt{S} = 7$ TeV, (1) is the direct production, (2) – from χ_{cJ} decays, (3) – from ψ' decays, (4) – sum of their all. For the different range in the rapidity: (a)- $2.0 < |y| < 2.5$, (b) - $2.5 < |y| < 3.0$, (c) - $3.0 < |y| < 3.5$

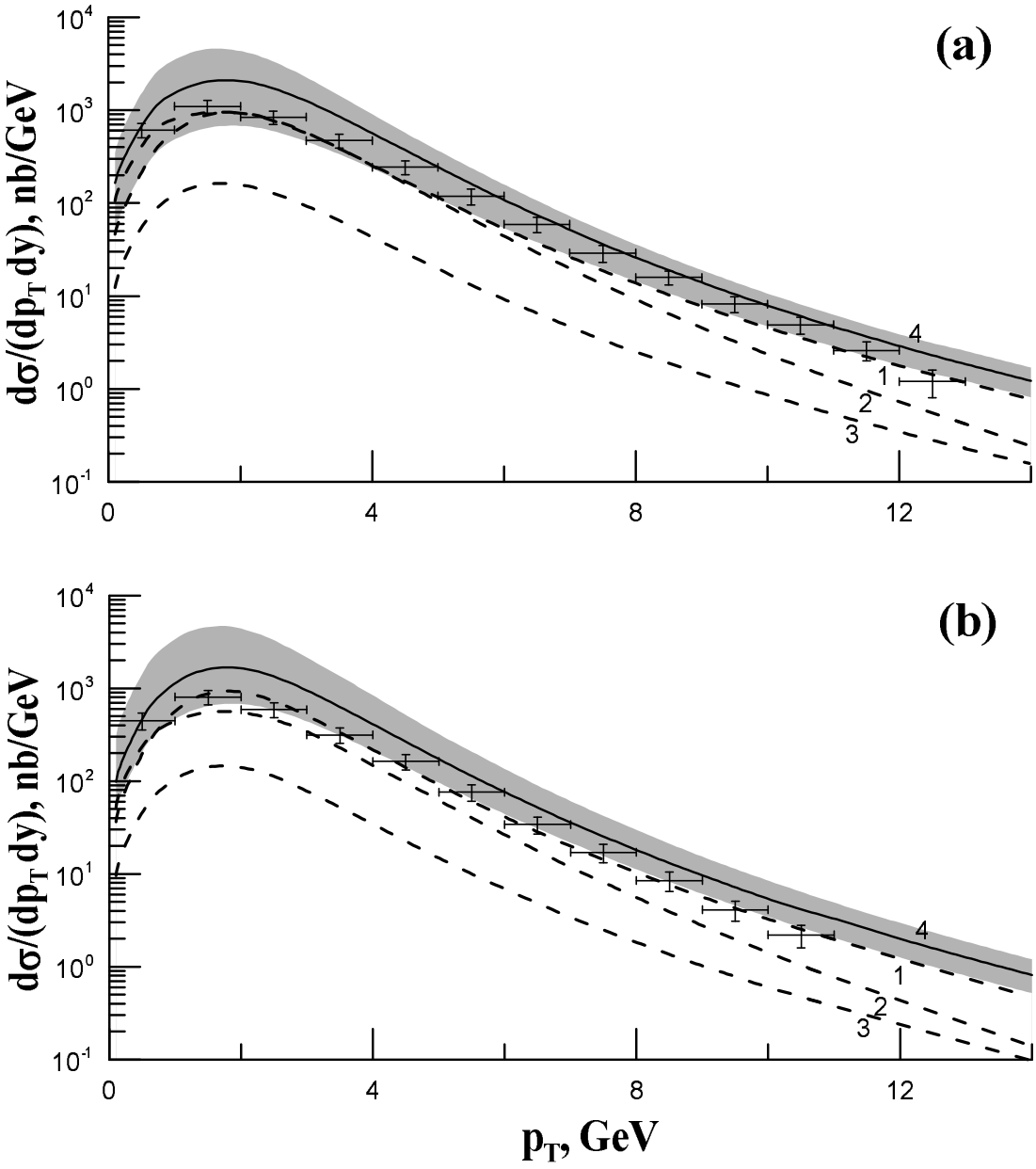

FIG. 9: Prompt J/ψ transverse momentum spectrum from LHCb Collaboration [18], $\sqrt{S} = 7$ TeV, (1) is the direct production, (2) – from χ_{cJ} decays, (3) – from ψ' decays, (4) – sum of their all. For the different range in the rapidity: (a)– $3.5 < |y| < 4.0$, (b) – $4.0 < |y| < 4.5$

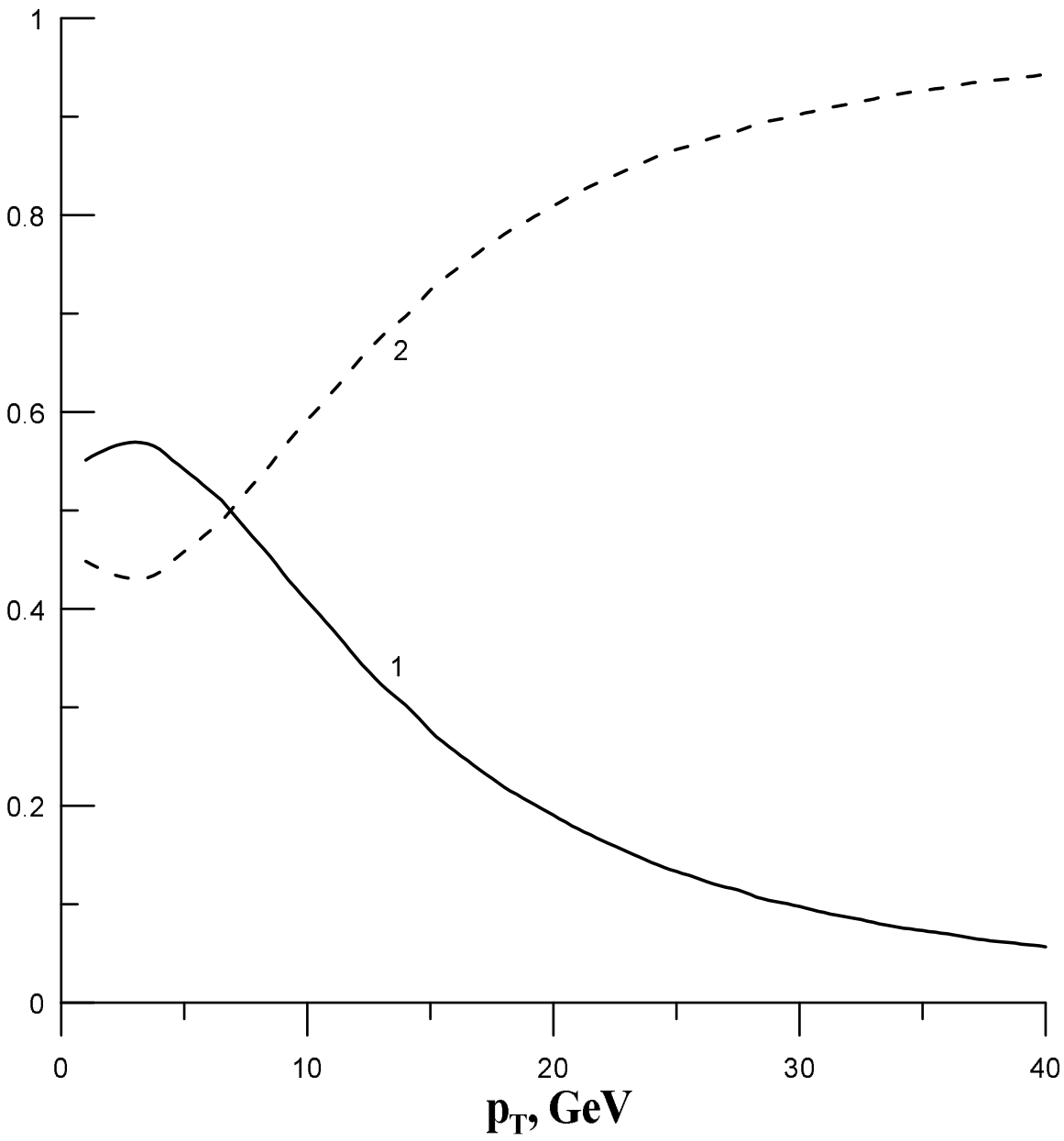

FIG. 10: The relative contributions of the color-singlet (curve 1) and color-octet (curve 2) production mechanisms to the prompt J/ψ transverse momentum spectrum at the $\sqrt{S} = 7$ TeV, $1.5 < |y| < 2.0$.